RSC Advances

PAPER

Cite this: *RSC Adv.*, 2020, **10**, 42128

The potential role of the 5,6-dihydropyridin-2(1*H*)-one unit of piperlongumine on the anticancer activity†

Wen-Wen Mu, Peng-Xiao Li, Yue Liu, Jie Yang* and Guo-Yun Liu*

Received 15th October 2020
Accepted 9th November 2020

DOI: 10.1039/d0ra08778e

rsc.li/rsc-advances

Piperlongumine (**PL**), a potent anticancer agent from the plant long pepper (*Piper longum*), contains the 5,6-dihydropyridin-2(1*H*)-one heterocyclic scaffold and cinnamoyl unit. In this paper, we synthesized a series of **PL** analogs and evaluated their cytotoxicity against cancer cells for the sake of exploring which pharmacophore plays a more potent role in enhancing the anticancer activities of **PL**. These results illustrated that the position effect, not the electronic effect, of substituents plays a certain role in the cytotoxicity of **PL** and its analogs. More important, the 5,6-dihydropyridin-2(1*H*)-one unit, a potent pharmacophore in enhancing the antiproliferative activities of **PL**, could react with cysteamine and lead to ROS generation, and then bring about the occurrence of ROS-induced downstream events, followed by cell cycle arrest and apoptosis. This work suggests that introducing a lactam unit containing Michael acceptors may be a potent strategy to enhancing the anticancer activity of drugs.

Introduction

The lactam ring scaffold, arguably one of the most acknowledged nitrogen-containing heterocycles studied so far, has attracted much attention in the fields of chemistry, biology and medicine.[1–3] Lactams, containing four-membered heterocycles,[4] five-membered heterocycles,[5] six-membered heterocycles[6] and so on, have been used extensively as potent substrates for various types of bioactive molecules. β-Lactam derivatives, initially focusing on their antibacterial properties,[7] have shown diverse pharmacological activities like anticancer,[4] anti-inflammatory[8] and anti-HIV activity.[9] 5,6-Dihydropyridin-2(1*H*)-one, an essential six-membered lactam derivative, is a potent pharmacophore in many naturally occurring medicines. Drugs containing the 5,6-dihydropyridin-2(1*H*)-one moiety are of great importance because they have been proven to show significant antifungal,[10] antidiabetic[11] and anticancer[12] activities.

Piperlongumine (**PL**), a naturally occurring alkaloid from the plant long pepper (*Piper longum*), is chemically characterized by the presence of the 5,6-dihydropyridin-2(1*H*)-one heterocyclic scaffold and cinnamoyl pharmacophore.[5] **PL** has been reported to possess multiple pharmacological effects including anti-inflammatory,[13] anti-platelet,[14] anti-bacterial,[15] and especially, anticancer properties.[6] The antineoplastic activities of **PL** have been noted in a number of cancer cell lines and a variety of animal models.[16,17] Moreover, **PL** has also been found to induce cell death by both caspase-dependent apoptosis and necrosis.[17,18] Additionally, **PL** could generally inhibit PI3K/Akt/mTOR signaling pathway[18] and glutathione S-transferase π (GSTπ), followed by disrupting the redox homeostasis and boosting the reactive oxygen species production in cancer cells.[19]

α,β-Unsaturated ketones, typically found in **PL**, curcuminoids, cinnamic acids derivatives, could significantly improve the pharmacological properties and have been a novel design concept of covalent drugs.[20] α,β-Unsaturated ketones were usually prepared through the Claisen–Schmidt reaction of acetone with aldehydes. Zhang *et al.* developed a more effective method for synthesizing α,β-unsaturated ketones by using proline-modified catalyst under very mild and green conditions.[21] Moreover, Zhang *et al.* also reported a gram-scale protocol for the synthesis of dialkylideneacetones, which was a very reliable and practical method in laboratory and at the industrial level.[22]

However, many efforts have been placed in the synthesizing **PL** analogs and exploring their mechanisms against cancer cells, the two pharmacophore, 5,6-dihydropyridin-2(1*H*)-one heterocyclic scaffold and cinnamoyl unit, which plays a more potent role on enhancing the anticancer activities of **PL** still need to be explored. Therefore, we design and synthesized a series of **PL** analogs (Scheme 1), and evaluated their cytotoxicity against cancer cells. Thus we focus on the structure–activity relationship (SAR) from the perspective of chemistry and explore the apoptotic mechanism associated with **PL** analogs.

School of Pharmacy, Liaocheng University, 1 Hunan Street, Liaocheng, Shandong 252000, China. E-mail: yangjie1110@163.com; guoyunliu@126.com; Tel: +86 15063505132

† Electronic supplementary information (ESI) available. See DOI: 10.1039/d0ra08778e

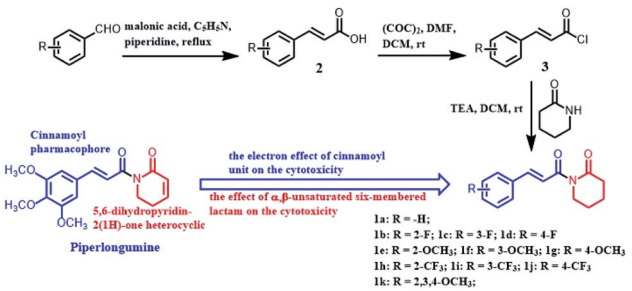

Scheme 1 Molecular structures and synthetics routs of piperlongumine analogs.

Experimental section

Materials

Roswell Park Memorial Institute (RPMI)-1640 was from Hyclone. 3-(4,5-Dimethylthiazol-2-yl)-2,5-diphenyltetrazolium bromide (MTT), rhodamine 123, 2′,7′-dichlorofluorescein diacetate, *N*-acetylcysteine (NAC), GSH and GSSG Assay kit, and thiobarbituric acid were purchased from Beyotime. Annexin V-FITC/PI apoptosis detection kit was from BD Biosciences. Substituted benzaldehyde, malonic acid, 2-piperidone and piperlongumine were from Energy Chemical. All other chemicals were of the highest quality available.

Synthesis of the PL analogs

General procedure for the synthesis of substituted cinnamic acids. The substituted cinnamic acids were synthesized according to the published procedure.[5] Briefly, the corresponding aldehyde (20 mmol), malonic acid (24 mmol) and piperidine (1.2 mL) were dissolved in pyridine (12 mL) and refluxed for 3 h. After cooling in an ice bath, the solid were filtered and recrystallized from ethanol to afford the corresponding acids.

General procedure for the synthesis of piperlongumine analogs. The mixture, containing oxalyl chloride (6 mmol), a catalytic amount of DMF (0.01 equiv.), the substituted cinnamic acids (2 mmol) and dry CH_2Cl_2 (4 mL), was stirred at room temperature for 24 h. After removing the solvent, the residue, triethylamine (6 mmol) and lactam (2.4 mmol) was dissolved in dry CH_2Cl_2 (5 mL), and stirred at room temperature for 24 h before extracting with ethyl acetate. Then the crude products were purified with a silica gel column.[5] Their structures were confirmed by ^{1}H and ^{13}C NMR spectroscopy.

(E)-1-(3-(3-Phenyl)acryloyl)piperidine-2-one ***(1a).*** Yield 33.8%, white solid, ^{1}H NMR (500 MHz, $CDCl_3$), δ 7.72 (d, J = 15.5 Hz, 1H), 7.58–7.56 (m, 2H), 7.46 (d, J = 15.5 Hz, 1H), 7.37–7.36 (m, 3H), 3.82–3.79 (m, 2H), 2.62–2.60 (m, 2H), 1.90–1.87 (m, 4H); ^{13}C NMR (125 MHz, $CDCl_3$), δ 173.9, 169.7, 143.2, 135.2, 130.0, 128.8, 128.3, 122.1, 44.60, 34.9, 22.6, 20.6; HRMS *m*/*z* (ES^+): $[M + Na]^+$ 252.0951 (theor 252.1000).

(E)-1-(3-(2-Fluorinephenyl)acryloyl)piperidine-2-one ***(1b).*** Yield 26.5%, white solid, ^{1}HNMR (500 MHz, $CDCl_3$), δ 7.84 (d, J = 16.0 Hz, 1H), 7.60 (t, J = 7.5 Hz, 1H), 7.50 (d, J = 16.0 Hz, 1H), 7.35–7.30 (m, 1H), 7.13 (t, J = 7.5 Hz, 1H), 7.09–7.05 (m, 1H), 3.82–3.79 (m, 2H), 2.62–2.59 (m, 2H), 1.90–1.87 (m, 4H); ^{13}C NMR (125 MHz, $CDCl_3$), δ 172.8, 168.5, 161.4, 134.2, 130.3, 128.0, 123.4, 123.3, 122.3, 115.1, 43.6, 33.9, 21.5, 19.6; HRMS *m*/*z* (ES^+): $[M + Na]^+$ 270.0852 (theor 270.0906).

(E)-1-(3-(3-Fluorinephenyl)acryloyl)piperidine-2-one ***(1c).*** Yield 36.2%, yellow solid, ^{1}HNMR (500 MHz, $CDCl_3$), δ 7.64 (d, J = 16.0 Hz, 1H), 7.43 (d, J = 16.0 Hz, 1H), 7.34–7.32 (m, 2H), 7.26–7.25 (m, 1H), 7.07–7.03 (m, 1H), 3.81–3.79 (m, 2H), 2.63–2.60 (m, 2H), 1.91–1.88 (m, 4H); ^{13}C NMR (125 MHz, $CDCl_3$), δ 173.9, 169.4, 164.0, 141.5, 137.5, 130.3, 124.2, 123.5, 116.9, 114.5, 44.7, 34.9, 22.5, 20.6; HRMS *m*/*z* (ES^+): $[M + Na]^+$ 270.0852 (theor 270.0906).

(E)-1-(3-(4-Fluorinephenyl)acryloyl)piperidine-2-one ***(1d).*** Yield 23.1%, white solid, ^{1}H NMR (500 MHz, $CDCl_3$), δ 7.68 (d, J = 15.5 Hz, 1H), 7.56–7.53 (m, 2H), 7.39 (d, J = 15.5 Hz, 1H), 7.05 (t, J = 8.5 Hz, 2H), 3.81–3.79 (m, 2H), 2.62–2.59 (m, 2H), 1.90–1.87 (m, 4H); ^{13}C NMR (125 MHz, $CDCl_3$), δ 173.9, 169.5, 164.8, 141.9, 131.4, 130.1, 121.9, 116.0, 44.6, 34.9, 22.6, 20.6; HRMS *m*/*z* (ES^+): $[M + Na]^+$ 270.0856 (theor 270.0906).

(E)-1-(3-(2-Methoxylphenyl)acryloyl)piperidine-2-one ***(1e).*** Yield 58.4%, white solid, ^{1}H NMR (500 MHz, $CDCl_3$), δ 8.07 (d, J = 15.5 Hz, 1H), 7.59 (d, J = 7.5 Hz, 1H), 7.51 (d, J = 16.0 Hz, 1H), 7.32–7.30 (m, 1H), 6.94 (t, J = 7.5 Hz, 1H), 6.90 (d, J = 8.5 Hz, 1H), 3.88 (s, 3H), 3.81–3.79 (m, 2H), 2.61–2.59 (m, 2H), 1.89–1.86 (m, 4H); ^{13}C NMR (125 MHz, $CDCl_3$), δ 173.8, 170.1, 158.4, 138.6, 131.2, 128.8, 124.2, 122.4, 120.6, 111.1, 55.5, 44.6, 34.9, 22.6, 20.7; HRMS *m*/*z* (ES^+): $[M + Na]^+$ 282.1048 (theor 282.1106).

(E)-1-(3-(3-Methoxylphenyl)acryloyl)piperidine-2-one ***(1f).*** Yield 30.4%, white solid, ^{1}H NMR (500 MHz, $CDCl_3$), δ 7.68 (d, J = 15.5 Hz, 1H), 7.44 (d, J = 15.5 Hz, 1H), 7.29 (d, J = 7.5 Hz, 1H), 7.17 (d, J = 7.5 Hz, 1H), 7.08–7.07 (m, 1H), 6.92–6.90 (m, 1H), 3.83 (s, 3H), 3.81–3.79 (m, 2H), 2.62–2.59 (m, 2H), 1.90–1.87 (m, 4H); ^{13}C NMR (125 MHz, $CDCl_3$), δ 173.8, 169.6, 159.9, 143.1, 136.5, 129.7, 122.4, 121.0, 116.0, 113.1, 55.3, 44.6, 34.9, 22.6, 20.6; HRMS *m*/*z* (ES^+): $[M + Na]^+$ 282.1055 (theor 282.1106).

(E)-1-(3-(4-Methoxylphenyl)acryloyl)piperidine-2-one ***(1g).*** Yield 63.4%, yellow solid, ^{1}H NMR (500 MHz, $CDCl_3$), δ 7.70 (d, J = 15.5 Hz, 1H), 7.53 (d, J = 9.0 Hz, 2H), 7.37 (d, J = 15.5 Hz, 1H), 6.89 (d, J = 9.0 Hz, 2H), 3.83 (s, 3H), 3.80–3.78 (m, 2H), 2.61–2.58 (m, 2H), 1.89–1.86 (m, 4H); ^{13}C NMR (125 MHz, $CDCl_3$), δ 173.8, 169.8, 161.2, 143.3, 130.0, 127.9, 119.7, 114.2, 55.4, 44.5, 35.0, 22.6, 20.6; HRMS *m*/*z* (ES^+): $[M + Na]^+$ 282.1057 (theor 282.1106).

(E)-1-(3-(2-Trifluoromethylphenyl)acryloyl)piperidine-2-one ***(1h).*** Yield 17.5%, yellow solid, ^{1}H NMR (500 MHz, $CDCl_3$), δ 8.04 (d, J = 15.5 Hz, 1H), 7.80 (d, J = 8.0 Hz, 1H), 7.69 (d, J = 7.5 Hz, 1H), 7.54 (t, J = 7.5 Hz, 1H), 7.46–7.39 (m, 2H), 3.83–3.80 (m, 2H), 2.62–2.59 (m, 2H), 1.91–1.88 (m, 4H); ^{13}C NMR (125 MHz, $CDCl_3$), δ 173.9, 168.9, 137.9, 134.2, 132.0, 129.2, 128.2, 126.3, 126.0, 126.0, 44.6, 34.9, 22.5, 20.6; HRMS *m*/*z* (ES^+): $[M + Na]^+$ 320.0817 (theor 320.0874).

(E)-1-(3-(3-Trifluoromethylphenyl)acryloyl) piperidine-2-one ***(1i).*** Yield 20.0%, white solid, ^{1}H NMR (500 MHz, $CDCl_3$), δ 7.78 (s, 1H), 7.73 (d, J = 8.0 Hz, 1H), 7.69 (d, J = 15.5 Hz, 1H), 7.61 (d, J = 7.5 Hz, 1H), 7.51–7.45 (m, 2H), 3.82–3.80 (m, 2H), 2.64–2.61 (m, 2H), 1.91–1.88 (m, 4H); ^{13}C NMR (125 MHz, $CDCl_3$), δ 173.9,

169.3, 141.0, 136.0, 131.3, 129.3, 126.3, 124.7, 124.0, 44.7, 34.9, 22.5, 20.6; HRMS *m*/*z* (ES^+): $[M + Na]^+$ 320.0817 (theor 320.0874).

*(E)-1-(3-(4-Trifluoromethylphenyl)acryloyl)piperidine-2-one (**1j**).* Yield 62.5%, white solid, ^1H NMR (500 MHz, $CDCl_3$), δ 7.69–7.61 (m, 5H), 7.51 (d, $J = 16.0$ Hz, 1H), 3.83–3.81 (m, 2H), 2.64–2.61 (m, 2H), 1.91–1.89 (m, 4H), ^{13}C NMR (125 MHz, $CDCl_3$), δ 173.9, 169.2, 140.8, 138.6, 128.3, 125.7, 124.7, 44.7, 34.9, 22.5, 20.6; HRMS *m*/*z* (ES^+): $[M + Na]^+$ 320.0823 (theor 320.0874).

*(E)-1-(3-(3,4,5-Trimethoxylphenyl)acryloyl) piperidine-2-one (**1k**).* Yield 55.7%, yellow solid, ^1H NMR (500 MHz, $CDCl_3$), δ 7.64 (d, $J = 15.5$ Hz, 1H), 7.37 (d, $J = 15.5$ Hz, 1H), 6.78 (s, 2H), 3.88 (s, 6H), 3.87 (s, 3H), 3.81–3.78 (m, 2H), 2.62–2.59 (m, 2H), 1.89–1.87 (m, 4H); ^{13}C NMR (125 MHz, $CDCl_3$), δ 173.9, 169.6, 153.4, 143.5, 140.0, 130.7, 121.3, 105.5, 61.0, 56.2, 44.6, 35.0, 22.6, 20.6; HRMS *m*/*z* (ES^+): $[M + Na]^+$ 342.1258 (theor 342.1317).

In vitro antiproliferative activity

Human lung cancer cells (A549), human ovarian cancer cells (SK-OV3), human normal liver cells (LO2) and human embryonic kidneys cells (293T) were purchased from the Shanghai Institute of Biochemistry and Cell Biology. The antiproliferative activities was performed by the MTT assay as reported previously.[23] Briefly, A549 (3×10^3 per well), SK-OV3 (5×10^3 per well), LO2 (5×10^3 per well) and 293T (5×10^3 per well) were plated in 96-well plates and incubated with vehicle alone or the tested compounds for 48 h before measuring.

Stability assay

The stability of piperlongumine and its analog **1k** in PBS buffer (100 mM) at 25 °C was monitored at their maximum absorbance for 120 min at 10 min intervals as described previously.[24]

Cell cycle and apoptosis analysis

A549 cells (3×10^5) were seeded in 6-well plates and treated with vehicle alone or the tested compounds for 15 h (for cell cycle analysis) or 18 h (for cell apoptosis analysis). Then, the cells were harvested, washed with PBS, labeled with PI or FITC Annexin-V and PI, and analyzed by using a flow cytometry as described previously[23]

Intracellular ROS assay

A549 (3×10^5) cells were plated in 6-well plates and incubated with the vehicle alone or the tested compounds for 6 h. Then, the cells were collected, stained with DCFH-DA at the dark, and subsequently analyzed with a flow cytometry as described previously.[23]

Measurement of GSH and GSSG levels

A549 (3×105 cells per well) cells treated with the vehicle alone or the tested compounds for 6 h. Then, the cells were collected, lysed and centrifugated, the supernatant was used to determine the level of GSH and GSSG using a GSH and GSSG Assay Kit.[24]

Measurement of lipid peroxidation

A549 cells (3×105 cells per well) were cultured in 6-well plates and incubated with the vehicle alone or the test compounds for 15 h before harvesting. Then, the cells were lysed and the supernatant were tested for assessment of the lipid peroxidation as previously described.[24]

Measurement of mitochondrial membrane potential

A549 cells (3×10^5 cells per well) were plated in 6-well plates and incubated with the vehicle alone or the test compounds for 15 h. Then, the cells were harvested, and stained with Rhodamine 123 before analyzing by a flow cytometry as previously reported.[23]

Electrophilicity assessment by a kinetic thiol assay

The reactions of **PL** and **1k** with cysteamine were carried out in Tris–HCl (100 mM, pH 7.4) and EDTA (2 mM)–ethanol (v/v, 2/1) under pseudo-first-order conditions.[25] The test compounds (50 μM) were mixed with 100-fold cysteamine at 25 °C, and monitored the decay of their wavelength maxima by using a TU-1950 UV-vis spectrophotometer. The second-order rate constants (k_2) were obtained by plotting the pseudo-first-order constants *vs.* [cysteamine].

Determination of the reaction site by ^1H NMR and HRMS

^1H NMR spectra of **PL** (30 mM in d_6-DMSO) after adding cysteamine (90 mM in d_6-DMSO) at set intervals (0, 1 h) were recorded using a Bruker AV 500 spectrometer. After incubation 3 days, the reaction products were monitored by HRMS (Acquity UPLC I-Class/Xevo G2-XS QTOF).[6]

Statistical analysis

The data are expressed as the mean ± S.D. of at least three independent experiments. Data were analyzed by use of SPSS software 17.0 (SPSS, Inc., Chicago, IL, USA). The difference between two groups was analyzed by one-way analysis of variance (ANOVA) followed by Dunnett test (compare all drug treatment groups *vs.* control). The values were considered significant at $P < 0.05$. *: $P < 0.05$; **: $P < 0.01$; ***: $P < 0.001$ compared with control.

Results and discussion

Synthesis

Compounds **1a–k** were synthesized according to the synthetic route illustrated in Scheme 1. Firstly, the appropriate benzaldehyde was condensed with malonic acid in pyridine to afford the key intermediate **2**. Then compound 2 reacted with oxalyl chloride in dry CH_2Cl_2 to afford intermediate **3**, followed by a nucleophilic substitution reaction with 2-piperidone to generate crude products. The title compounds **1a–k** were obtained with medium yields after purification by column chromatography. All compounds were characterized by ^1H NMR and ^{13}C NMR.

Table 1 Cytotoxicity of PL and its analogs against A549 and SKOV3 cells[a]

Comps	IC_{50}/(μM)		Comps	IC_{50}/(μM)	
	A549	SKOV3		A549	SKOV3
	161.1 ± 5.4	186.7 ± 11.6	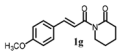	>200	>200
	138.6 ± 9.2	92.5 ± 4.3		191.0 ± 6.1	>200
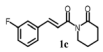	171.8 ± 9.2	72.8 ± 2.3	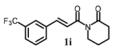	132.3 ± 8.2	>200
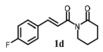	178.1 ± 13.2	177.4 ± 7.8	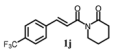	160.9 ± 1.4	>200
	>200	191.0 ± 4.8	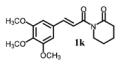	115.2 ± 1.1	>200
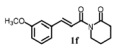	143.3 ± 13.8	83.8 ± 1.9	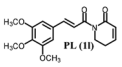	7.9 ± 0.8	19.4 ± 1.7

[a] The IC_{50} value is the concentration of a compound tested to cause 50% inhibition of cell viability after 48 h of treatment, and is expressed as the mean ± SD for three determinations.

Cytotoxicity and SAR

The antiproliferative activities of **PL** and its analogs (**1a–k**) were evaluated against A549 and SKOV3 cells by the MTT assay, and the results were listed in Table 1. In general, the cell-killing effects of all the **PL** analogs (**1a–k**) were much lower than **PL**. As a comparision, compounds with electron-donating groups (–OCH_3) exhibited nearly equivalent cytotoxicity to the compounds with electron-withdrawing groups (–F, –CF_3), suggesting that the electronic effect of substituents are not necessary for the antiproliferative activities of **PL** and its analogs. Whereas, the compounds with *meta*-substituents (**1c**, **1f**, **1i**) were more active than their corresponding *ortho*- and *para*-substituted compounds. Compound **1f** (*meta*-methoxyl group, IC_{50} = 143.3 and 83.8 μM in A549 and SKOV3 cells, respectively) showed stronger cytotoxicity than compounds **1e** (*ortho*-methoxyl group, IC_{50} > 200 and = 191.0 μM in A549 and SKOV3 cells, respectively) and **1g** (*para*-methoxyl group, IC_{50} > 200 μM in both A549 and SKOV3 cells). This result indicated that the position effect of substituents play a certain role on the cytotoxicity of **PL** and its analogs. This phenomenon may be attributed to the stereostructures of *meta*-substituted compounds, which are favour of binding certain protein in cells, such as thioredoxin reductase (TrxR), carbonic anhydrase and so on.[6]

In addition, the antiproliferative activity of **1c** against SKOV3 was much higher than that of compound **1k**. This result hinted that the cytotoxicity of **PL** analogs may be partly attributed to the cinnamoyl pharmacophore, and the rational modification of cinnamoyl unit might be conduce to increase their anticancer activity. For example, the cinnamic acid–progenone hybrids, with 3-OH or 4-OH cinnamoyl unit, exhibited more activity towards A549 and HL-60 cells than corresponding methoxyl-hybrids.[26] Gaikwad *et al.* deduced that cinnamamides with electron-withdrawing groups at the para position were important for their anticancer activity.[27] The 4-methylcinnamic acid unit has the ability to remarkably improve the inhibition activity of oleanolic acid–cinnamic acid ester derivatives against MCF-7 cells.[28]

More important, in comparison with the parent **PL**, all the **PL** analogs, lacking of the 5,6-dihydropyridin-2(1*H*)-one heterocyclic scaffold, displayed much lower cytotoxicity (Table 1). Specially, compound **1k** exhibited the less antiproliferative activities against A549 and SKOV3 cells with the IC_{50} values of 115.2 and greater than 200 μM, respectively. Additionally, the stability of **PL** and its analog **1k** in PBS buffer were determined. As shown in Fig. 1, no apparent changes were observed in the case of **PL** and **1k**. The above results clearly indicated that the 5,6-dihydropyridin-2(1*H*)-one pharmacophore play a potent role on the antiproliferative activities of **PL** and its analogs. As far as the 5,6-dihydropyridin-2(1*H*)-one pharmacophore is concerned, it is a potent strategy to increase the activity by introducing the pharmacophore into drug molecules. Moreover, some previous studies have shown that **PL** selectively kill cancer cells without damaging certain normal cells, such as astrocyte, breast epithelial (76N), keratinocytes (HKC) cells and so on.[29,30] Unexpectedly, compared with cancer cells, **PL** and **1k** displayed no obvious selectivity of cytotoxicity against normal cells (LO2 and

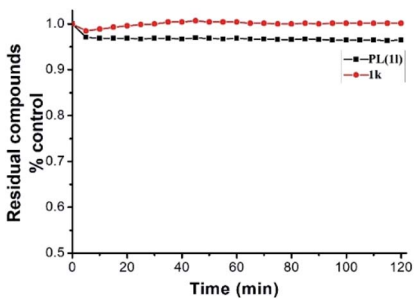

Fig. 1 Stability assessment on PL (50 μM) and its analog **1k** (50 μM) in PBS buffer (100 mM) at 25 °C by monitoring the decrease in their maximum absorbance.

Table 2 Cytotoxicity of PL and its analogs against LO2 and 293T cells

	IC_{50}/(μM)			IC_{50}/(μM)	
Comp.	LO2	293T	Comp.	LO2	293T
PL (**1l**)	10.4 ± 0.3	7.5 ± 0.4	**1k**	>200	182.6 ± 1.8

293T cells) (Table 2). As listed in Table 2, **PL** exhibited the antiproliferative activities against normal LO2 and 293T cells with the IC_{50} values of 10.4 and 7.5 μM, respectively.

Cell cycle and apoptosis study by flow cytometry

To investigate the possible mechanisms underlying the antiproliferative activities, we further determined the effects of **PL** and **1k** on cell cycle arrest and apoptosis by flow cytometry. As shown in Fig. 2A, 15 h of treatment with **PL** arrested cell cycle at G2/M phase in a dose-dependent manner. Increasing concentration from 10 to 30 μM led to a successive increase of G2/M phase cell population from 20.0% (control) to 33.8% (30 μM). Additionally, after 18 h treatment, the number of apoptotic A549 cells was strikingly increased with increasing concentrations (10, 20 and 30 μM) of **PL** (Fig. 2B). For example, 30 μM **PL** caused 22.7% apoptosis of the total cell count. In contrast, 100 μM **1k** displayed no obvious effect on both the cell cycle arrest and induction of apoptosis (Fig. 2A and B). Moreover, pretreatment with *N*-acetylcysteine (NAC), a potent antioxidant, noticeably reversed the cell cycle arrest and apoptosis induced by **PL** (Fig. 2A and B), preliminarily suggesting the involvement of reactive oxygen species.

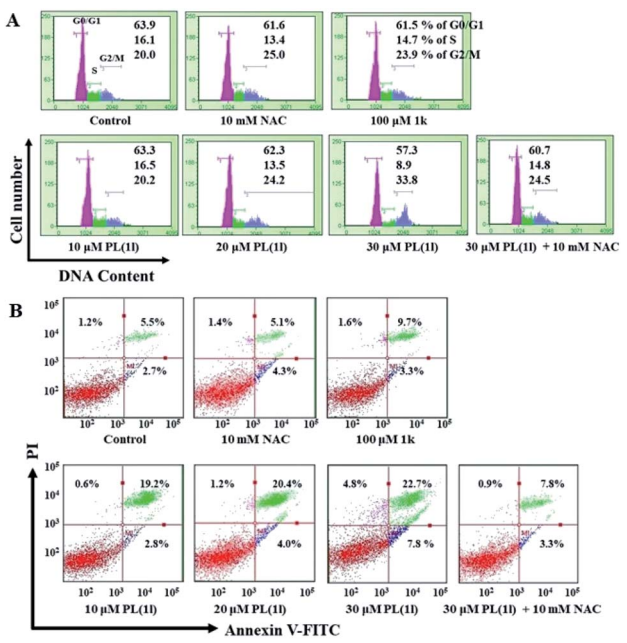

Fig. 2 The effect of PL and its analog **1k** on the cell cycle arrest (A) and apoptosis (B) in A549 cells. Cells were treated with PL and **1k** at the indicated concentrations for 15 h (in cell cycle analysis) and 18 h (in cell apoptosis analysis) in the absence or presence of NAC. Data are representative of three independent experiments.

ROS accumulation and ROS-induced downstream events

ROS generation has been implicated as an upstream signal that could bring about signaling transduction culminating in apoptosis.[31] Based on the above results, we initially deem that the ROS production should be a potent mechanism underlying the antiproliferative activities of **PL**. Therefore, we next determined the ROS accumulation using DCFH-DA, a widely used oxidation-sensitive probe to measure intracellular ROS levels.[32] As shown in Fig. 3A, 6 h treatment with **PL** induced an apparent intracellular ROS accumulation in a dose-dependent manner. The fluorescence intensity measured in cells treated with 30 μM **PL** were increased by approximately 1.7-fold compared with the vehicle control. In contrast, 100 μM **1k** exhibited almost no ROS-generating ability under the same conditions. As expected, pretreatment with NAC, an effective antioxidant, the ROS induced by 30 μM **PL** were almost completely abolished (Fig. 3A), in line with the results obtained by the cell cycle and apoptosis analysis. This result also suggested that the ROS generation induced by **PL** may be related with its cytotoxicity, cell cycle arrest and apoptotic activities.

The ratio of GSH/GSSG, a characteristic of intracellular redox balance, could be vulnerable to change by the sustained flux of ROS.[33] Therefore, we determined the redox balance in A549 cells to ascertain whether the ROS accumulation induced by **PL** resulted in an imbalance of intracellular redox state. As shown in Fig. 3B, the ratios of GSH/GSSG were sharply decreased and exhibited an excellent dose-dependent fashion. The redox imbalance induced by 100 μM **1k** was equal to that induced by 20 μM **PL**. Expectly, pretreatment with NAC, the redox imbalance induced by 30 μM **PL** was effectively prevent.

Additionally, the sustained flux of ROS could be susceptible to attack plasma membrane and result in lipid peroxidation.[32] Thus, we measured the amount of malondialdehyde (MDA), the biomarker of lipid peroxidation, by using thiobarbituric acid-reactive substance. After exposed to **PL** for 15 h, a dose-dependent increase for the MDA levels in cells was observed (Fig. 3C). Treatment with 30 μM **PL**, the level of MDA were increased by about 3-fold compared with the vehicle control. In

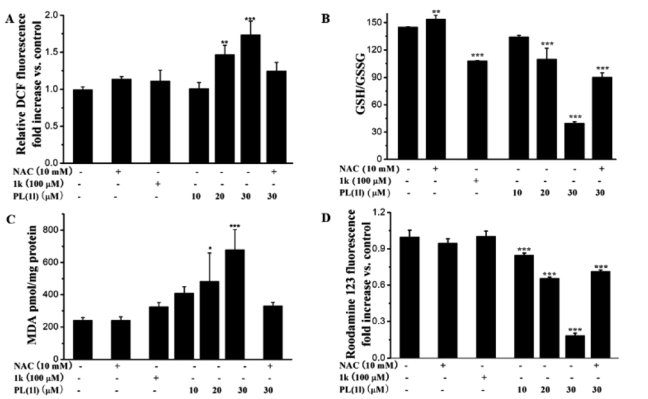

Fig. 3 The effects of PL on the ROS accumulation (A) and ROS-induced downstream events (B) the redox imbalance; (C) lipid peroxidation; (D) the loss of MMP.

contrast, 100 μM **1k** was less active in changing the MDA levels (Fig. 3C). And pretreatment with NAC also abolished the lipid peroxidation induced by 30 μM **PL**, supporting the lipid peroxidation was associated with ROS production.

The excess ROS could damage the functions of mitochondrial, which playing a dominant role in the regulation of cell survival.[34] We subsequently determined the loss of mitochondrial membrane potential (MMP) using rhodamine 123 by flow cytometry. As shown in Fig. 3D, we found that **PL** triggered an obvious decrease in the collapse of MMP in a dose-dependent fashion. Moreover, 30 μM **PL** caused an 80% decrease of MMP in A549 cells compared with the vehicle control, and the decrease was significantly blocked by pretreatment with NAC.

Based on the above results, we found that **PL** could cause the generation of ROS, a signal molecule to modulate various biological processes,[32] and lead to the occurence of ROS-induced downstream events, such as redox imbalance, lipide peroxidation and the loss of MMP. In addition, the antioxidant of NAC could effectively block the damages induced by **PL** in A549 cells.

Electrophilicity assessment and determination of the reaction site of PL

Drugs, containing Michael acceptor, could irreversibly inhibit the TrxR and trigger ROS generation. Piperlongumine (**PL**) contains two Michael acceptor units, 5,6-dihydropyridin-2(1*H*)-one heterocyclic scaffold and cinnamoyl pharmacophore. In order to ascertain which pharmacophore plays a more potent role on enhancing the anticancer activities of **PL**, we assessed the electrophilicity of **PL** and its analog **1k** by measuring their second-order rate constants with cysteamine. On the basis of the k_2 values (Table 3), the electrophilicity of **PL** ($k_2 = 2.26\ M^{-1}\ s^{-1}$) was much higher than its analog **1k** ($k_2 = 1.80\ M^{-1}\ s^{-1}$). The result indeed accord with their cytotoxicity and proapoptotic activities. The results of electrophilicity and cytotoxicity also hinted that the cinnamoyl unit of **PL** showed a certain chemical reactivity toward cysteamine, and the 5,6-dihydropyridin-2(1*H*)-one heterocyclic scaffold was crucial to the cytotoxicity, proapoptotic activities, ROS accumulation and ROS-induced downstream events.

To identify the specific site for the reaction of **PL** with cysteamine, the ^{1}H NMR spectroscopy changes of **PL** in the presence of three equivalents of cysteamine were also monitored in d_6-DMSO. The doublet at δ 6.974 (H-1 and H-1′) was the protons of the aromatic nucleus (Fig. 4A), and the integral was calibrated to 2.00 hydrogen. After incubating a mixture of **PL** and cysteamine for **1h**, the doublet integral of the olefinic proton at δ 5.965 (H-4) decreased from 1.00 to 0.12, and a weaker doublet appeared at δ 5.917 with the integral increasing from 0.00 to 0.03 (Table 4). This result illustrated that cysteamine was mainly added to the 5,6-dihydropyridin-2(1*H*)-one heterocyclic unit, and suggested that the α,β-unsaturated ketone of 5,6-dihydropyridin-2(1*H*)-one heterocyclic unit was more vulnerable to attack by cysteamine than that of cinnamoyl pharmacophore. Additionally, the HRMS analysis showed that the 1 : 1 and 1 : 2 adducts (*m*/*z*: 417.1466 and 494.1611, respectively) were formed between **PL** and cysteamine after 3 days of incubation (Fig. 4B).

Table 3 Second-order rate constants (k_2) for the reaction of **PL** and its analog **1k** with cysteamine at 25 °C[a]

Comp.	k_2 ($M^{-1}\ s^{-1}$)	Comp.	k_2 ($M^{-1}\ s^{-1}$)
PL (**1l**)	2.26 ± 0.04	**1k**	1.80 ± 0.08

[a] Reactions were carried out in Tris–HCl (100 mM, pH 7.4) and EDTA (2 mM)–ethanol (v/v, 2/1) under pseudo-first-order conditions. Data are expressed as the mean ± SD for three determinations.

The anticancer mechanism of PL and its analogs against A549 cells

ROS, a class of unstable chemically reactive, are ubiquitous common by-products in the process of life such as mitochondrial metabolism and protein folding.[35] ROS also can be produced by NADPH oxidases, a family of enzymes that transfer electrons from NADPH to O_2 to generated ROS, not as by-products.[36] Cancer cells, which display increased ROS to maintain their phenotypes, are more rely on the "redox adaptation" mechanism compared with normal cells. Stimulating intracellular ROS to a toxicity threshold to induce cell death is one of the important strategy for treatment cancer.[6] A large number of chemotherapeutic drugs containing Michael acceptor, such as curcumin, **PL**, quinones and so on, are widely used for the treatment of cancer.[37] The Michael acceptor of chemotherapeutic agents can irreversibly inhibit TrxR and trigger intracellular ROS accumulation.[6] As shown in Table 3, the reactive activity of **PL** with cysteamine was more than that of compound **1k**. Moreover, the Michael acceptor of lactam of **PL** analogs was the major reaction site of cysteamine (Fig. 4A). These results also hinted that the ROS generation induced by **PL** and **1k** (Fig. 3A) was major attributed to the electrophilicity of Michael acceptor of lactam of **PL**.

Apoptosis, programmed cell death, can be initiated by an intrinsic pathway or an extrinsic pathway. ROS are usually involved in both intrinsic and extrinsic pathways of apoptosis.[38] Extensive research has proved the potential of ROS in inducing apoptosis of cancer cells. **PL** substantially induced A549 cells apoptosis in a dose-dependent manner. Chemotherapeutic agents can inhibit the antioxidant defense systems or increase ROS production, which mediated activation of c-Jun N-terminal

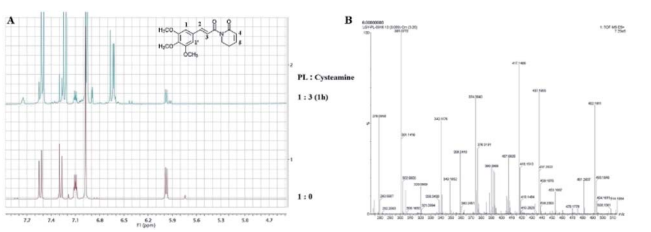

Fig. 4 Reaction of **PL** with cysteamine: (A) ^{1}H NMR spectra of **PL** in d_6-DMSO before and after adding cysteamine; (B) HRMS spectrum recorded 3 days after mixing **PL** with 3 eq. of cysteamine.

Table 4 Quantification of the analytes after the addition of cysteamine

Signals assigned	Chemical shift (ppm)	Coupled splitting	Coupling constants (*J*/Hz)	Time (h)	Integral	Sum of integral
H-1	6.974	s	—	0	2.00	2.00
H-1′	6.974–6.890	—	—	1	2.00	2.00
H-4	5.965	d	9.5	0	1.00	1.00
	5.965/5.917	d/d	9.5/9.5	1	0.12/0.03	0.15

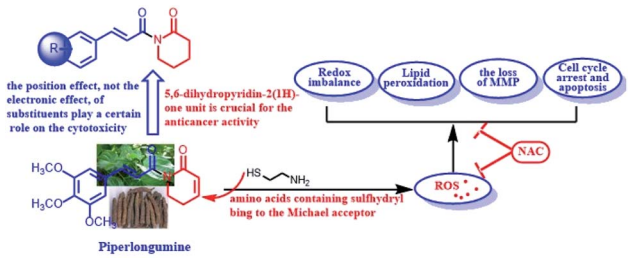

Scheme 2 The 5,6-dihydropyridin-2-(1*H*)-one unit is crucial for the anticancer activity.

kinases (JNK) pathway, inhibition of NF-κB activation and induction of mitochondrial dysfunction to promote cancer cell apoptosis. As shown in Fig. 3B, **PL** remarkably decrease the ratio of GSH/GSSG may be due to the irreversible inhibition of TrxR, and the redox imbalance induced by **1k** may be attributed to the GSH depletion. In addition, ROS accumulation could lead the oxidation of intracellular lipids and proteins. As illustrated in Fig. 3C, **PL** obviously induced lipid peroxidation in a dose-dependent fashion. **PL** also disrupted the MMP in a dose-dependent manner as illustrated in Fig. 3D. All of the above results, ROS accumulation, redox imbalance, lipid peroxidation, the loss of MMP and apoptosis, induced by **PL** can be reversed by pretreatment with NAC, a well known antioxidant. This phenomenon indicated that **PL** induced apoptosis of A549 cells through ROS-mediated pathway.

Conclusions

In conclusion, we synthesized a panel of **PL** analogs and evaluated their cytotoxicity against cancer cells. These results revealed that the position effect, not the electronic effect, of substituents played a certain role on the cytotoxicity of **PL** and its analogs. More important, the 5,6-dihydropyridin-2(1*H*)-one unit was a potent pharmacophore in enhancing the antiproliferative activities of **PL** and its analogs. **PL** triggered the ROS generation, and then disrupted the redox balance, induced lipid peoxidation, collapsed the mitochondrial membrane potential, led to cell cycle arrest and cell apoptosis. From the perspective of chemistry, the 5,6-dihydropyridin-2(1*H*)-one pharmacophore of **PL** could react with cysteamine or other amino acids containing sulfhydryl, leading to the ROS generation (Scheme 2). This work suggested that the lactam unit containing Michael acceptors was an potent pharmacophore in enhancing the anticancer activity of drugs.

Conflicts of interest

The authors declare that they have no conflict of interest.

Acknowledgements

This work was supported by the National Natural Science Foundation of China (Grant No. 81901420), Shandong Provincial Natural Science Foundation (Grant No. ZR2018LH022), the Open Project of Shandong Collaborative Innovation Centre for Antibody Drugs (Grant No. CIC-AD1822 and CIC-AD1824).

Note and references

1 C. R. Pitts and T. Lectka, Chemical synthesis of β-lactams: asymmetric catalysis and other recent advances, *Chem. Rev.*, 2014, **114**, 7930–7953.

2 S. S. Tang, A. Apisarnthanarak and L. Y. Hsu, Mechanisms of β-lactam antimicrobial resistance and epidemiology of major community- and healthcareassociated multidrug-resistant bacteria, *Adv. Drug Delivery Rev.*, 2014, **78**, 3–13.

3 A. Huttner, S. Harbarth, W. W. Hope, J. Lipman and J. A. Roberts, Therapeutic drug monitoring of the b-lactam antibiotics: what is the evidence and which patients should we be using it for?, *J. Antimicrob. Chemother.*, 2015, **70**, 3178–3183.

4 S. Ranjbari, M. Behzadi, S. Sepehri, M. D. Aseman, A. Jarrahpour, M. Mohkam, Y. Ghasemi, A. R. Akbarizadeh, S. Kianpour, Z. Atioğlu, N. Özdemir, M. Akkurt, S. M. Nabavizadeh and E. Turos, Investigations of antiproliferative and antioxidant activity of β-lactam morpholino-1,3,5-triazine hybrids, *Bioorg. Med. Chem.*, 2020, **28**, 115408.

5 S. J. Peng, B. X. Zhang, X. K. Meng, J. Yao and J. G. Fang, Synthesis of piperlongumine analogues and discovery of nuclear factor erythroid 2-related factor 2 (Nrf2) activators as potential neuroprotective agents, *J. Med. Chem.*, 2015, **58**, 5242–5255.

6 W. J. Yan, Q. Wang, C. H. Yuan, F. Wang, Y. Ji, F. Dai, X. L. Jin and B. Zhou, Designing piperlongumine-directed anticancer agents by an electrophilicity-based prooxidant strategy: a mechanistic investigation, *Free Radical Biol. Med.*, 2016, **97**, 109–123.

7 M. O'Driscoll, K. Greenhalgh, A. Young, E. Turos, S. Dickey and D. V. Lim, Studies on the antifungal properties of *N*-thiolated β-lactams, *Bioorg. Med. Chem.*, 2008, **16**, 7832–7837.

8 A. E. G. E. Amr, N. M. Sabry and M. M. Abdulla, Synthesis, reactions, and anti-inflammatory activity of heterocyclic systems fused to a thiophene moiety using citrazinic acid as synthon, *Monatsh. Chem.*, 2007, **138**, 699–707.

9 N. Borazjani, S. Sepehri, M. Behzadi, A. Jarrahpour, J. A. Rad, M. Sasanipour, M. Mohkam, Y. Ghasemi, A. R. Akbarizadeh, C. Digiorgio, J. M. Brunel, M. M. Ghanbari, G. Batta and E. Turos, Three-component synthesis of chromeno β-lactam hybrids for inflammation and cancer screening, *Eur. J. Med. Chem.*, 2019, **179**, 389–403.

10 A. Haga, H. Tamoto, M. Ishino, E. Kimura, T. Sugita, K. Kinoshita, K. Takahashi, M. Shiro and K. Koyama, Pyridone alkaloids from a marine-derived fungus, *Stagonosporopsis cucurbitacearum*, and their activities against azole-resistant *Candida albicans*, *J. Nat. Prod.*, 2013, **76**, 750–754.

11 D. A. Wacker, Y. Wang, M. Broekema, K. Rossi, S. O'Connor, Z. Hong, G. Wu, S. E. Malmstrom, C. P. Hung, L. LaMarre, A. Chimalakonda, L. Zhang, L. Xin, H. Cai, C. Chu, S. Boehm, J. Zalaznick, R. Ponticiello, L. Sereda, S.-. Han, R. Zebo, B. Zinker, C. E. Luk, R. Wong, G. Everlof, Y. X. Li, C. K. Wu, M. Lee, S. Griffen, K. J. Miller, J. Krupinski and J. A. Robl, Discovery of 5-Chloro-4-((1-(5-chloropyrimidin-2-yl)piperidin-4-yl)oxy)-1-(2-fluoro-4-(methylsulfonyl)phenyl) pyridin-2(1*H*)-one (BMS-903452), an Antidiabetic Clinical Candidate Targeting GPR119, *J. Med. Chem.*, 2014, **57**, 7499–7508.

12 J. F. Zhou, Z. X. Huang, X. Nie and C. Lv, Piperlongumine induces apoptosis and G(2)/M phase arrest in human osteosarcoma cells by regulating ROS/PI3K/Akt pathway, *Toxicol. in Vitro*, 2020, **65**, 104775.

13 S. Thatikonda, V. Pooladanda, D. K. Sigalapalli and C. Godugu, Piperlongumine regulates epigenetic modulation and alleviates psoriasis-like skin inflammation *via* inhibition of hyperproliferation and inflammation, *Cell Death Dis.*, 2020, **11**, 21.

14 V. Yadav, A. Krishnan and D. Vohora, A systematic review on *Piper longum* L.: Bridging traditional knowledge and pharmacological evidence for future translational research, *J. Ethnopharmacol.*, 2020, **247**, 112255.

15 Y. C. Yang, S. G. Lee, H. K. Kim, S. H. Lee and H. S. Lee, A piperidine amide extracted from *Piper longum* L. fruit shows activity against *Aedes aegypti* mosquito larvae, *J. Agric. Food Chem.*, 2002, **50**, 3765–3767.

16 D. P. Bezerra, C. Pessoa, M. O. Moraes, N. M. Alencar, R. O. Mesquita, M. W. Lima, A. P. Alves, O. D. Pessoa, J. H. Chaves, E. R. Silveira and L. V. Costa-Lotufo, *In vivo* growth inhibition of sarcoma 180 by piperlonguminine, an alkaloid amide from the Piper species, *J. Appl. Toxicol.*, 2008, **28**, 599–607.

17 D. P. Bezerra, F. O. Castro, A. P. Alves, C. Pessoa, M. O. Moraes, E. R. Silveira, M. A. Lima, F. J. Elmiro and L. V. Costa-Lotufo, *In vivo* growth-inhibition of Sarcoma 180 by piplartine and piperine, two alkaloid amides from Piper, *Braz. J. Med. Biol. Res.*, 2006, **39**, 801–807.

18 F. Wang, Y. Mao, Q. You, D. Hua and D. Cai, Piperlongumine induces apoptosis and autophagy in human lung cancer cells through inhibition of PI3K/Akt/mTOR pathway, *Int. J. Immunopathol. Pharmacol.*, 2015, **28**, 362–373.

19 C. Duan, B. Zhang, C. Deng, Y. Cao, F. Zhou, L. Wu, M. Chen, S. Shen, G. Xu, S. Zhang, G. Duan, H. Yan and X. Zou, Piperlongumine induces gastric cancer cell apoptosis and G2/M cell cycle arrest both *in vitro* and *in vivo*, *Tumour Biol.*, 2016, **37**, 10793–10804.

20 S. Krishnan, R. M. Miller, B. Tian, R. D. Mullins, M. P. Jacobson and J. Taunton, Design of Reversible, Cysteine-Targeted Michael Acceptors Guided by Kinetic and Computational Analysis, *J. Am. Chem. Soc.*, 2014, **136**, 12624–12630.

21 H. Zhang, M. T. Han, T. Chen, L. Xu and L. Yu, Poly(*N*-isopropylacrylamide-*co*-L-proline)-catalyzed Claisen–Schmidt and Knoevenagel condensations: unexpected enhanced catalytic activity of the polymer catalyst, *RSC Adv.*, 2017, **7**, 48214–48221.

22 H. Zhang, M. T. Han, C. G. Yang, L. Yu and Q. Xu, Gram-scale preparation of dialkylideneacetones through $Ca(OH)_2$-catalyzed Claisen–Schmidt condensation in dilute aqueous EtOH, *Chin. Chem. Lett.*, 2019, **30**, 263–265.

23 J. Yang, W. W. Mu and G. Y. Liu, Synthesis and evaluation of the anticancer activity of bischalcone analogs in human lung carcinoma (A549) cell line, *Eur. J. Pharmacol.*, 2020, **888**, 173396.

24 G. Y. Liu, Q. Zhai, J. Z. Chen, Z. Q. Zhang and J. Yang, 2,2′-Fluorine mono-carbonyl curcumin induce reactive oxygen species-mediated apoptosis in human lung cancer NCI-H460 cells, *Eur. J. Pharmacol.*, 2016, **786**, 161–168.

25 H. L. Shi, Y. Li, X. R. Ren, Y. H. Zhang, Z. Yang and C. Z. Qi, A novel quinazoline-based analog induces G2/M cell cycle arrest and apoptosis in human A549 lung cancer cells *via* a ROS-dependent mechanism, *Biochem. Biophys. Res. Commun.*, 2017, **486**, 314–320.

26 Y. X. Ge, Y. H. Wang, J. Zhang, Z. P. Yu, X. Mu, J. L. Song, Y. Y. Wang, F. Yang, N. Meng and C. S. Jiang, New Cinnamic Acid-Pregenolone Hybrids as Potential Antiproliferative Agents: Design, Synthesis and Biological Evaluation, *Steroids*, 2019, **152**, 1–9.

27 N. Gaikwad, S. Nanduri and Y. V. Madhavi, Cinnamamide: An Insight into the Pharmacological Advances and Structure–Activity Relationships, *Eur. J. Med. Chem.*, 2019, **181**, 1–24.

28 S. R. Wang, W. Yang, Y. Fan, W. Dehaen, Y. Li, W. Wang, Q. Zheng and Q. Huai, Design and Synthesis of the Novel Oleanolic Acid-Cinnamic Acid Ester Derivatives and Glycyrrhetinic Acid–Cinnamic Acid Ester Derivatives with Cytotoxic Properties, *Bioorg. Chem.*, 2019, **88**, 1–15.

29 J. M. Liu, F. Pan, L. Li, Q. R. Liu, Y. Chen, X. X. Xiong, K. Cheng, S. B. Yu, Z. Shi, A. C. H. Yu and X. Q. Chen, Piperlongumine selectively kills glioblastoma multiforme cells *via* reactive oxygen species accumulation dependent JNK and p38 activation, *Biochem. Biophys. Res. Commun.*, 2013, **437**, 87–93.

30 L. Raj, T. Ide, A. U. Gurkar, M. Foley, M. Schenone, X. Li, N. J. Tolliday, T. R. Golub, S. A. Carr and A. F. Shamji, Selective killing of cancer cells by a small molecule

targeting the stress response to ROS, *Nature*, 2011, **475**, 231–234.

31 G. Y. Liu, Y. Z. Sun, N. Zhou, X. M. Du, J. Yang and S. J. Guo, 3,3′-OH curcumin causes apoptosis in HepG2 cells through ROS-mediated pathway, *Eur. J. Med. Chem.*, 2016, **112**, 157–163.

32 H. Pelicano, D. Carney and P. Huang, ROS stress in cancer cells and therapeutic implications, *Drug Resist. Updates*, 2004, **7**, 97–110.

33 S. Galadari, A. Rahman, S. Pallichankandy and F. Thayyullathil, Reactive oxygen species and cancer paradox: to promote or to suppress?, *Free Radical Biol. Med.*, 2017, **104**, 144–164.

34 A. B. Kunnumakkara, P. Anand and B. B. Aggarwal, Mobilized $CD34^{+}$ cells as a biomarker candidate for the efficacy of combined maximal tolerance dose and continuous infusional chemotherapy and G-CSF surge in gastric cancer, *Cancer Lett.*, 2008, **269**, 199–225.

35 H. Sies and D. P. Jones, Reactive oxygen species (ROS) as pleiotropic physiological signalling agents, *Nat. Rev. Mol. Cell Biol.*, 2020, **21**, 363–383.

36 T. F. Brewer, F. J. Garcia, C. S. Onak, K. S. Carroll and C. J. Chang, Chemical approaches to discovery and study of sources and targets of hydrogen peroxide redox signaling through NADPH oxidase proteins, *Annu. Rev. Biochem.*, 2015, **84**, 765–790.

37 J. M. Zhang, D. Z. Duan, Z. L. Song, T. Y. Liu, Y. N. Hou and J. G. Fang, Small molecules regulating reactive oxygen species homeostasis for cancer therapy, *Med. Res. Rev.*, 2020, 1–53.

38 T. Ozben, Oxidative stress and apoptosis: impact on cancer therapy, *J. Pharm. Sci.*, 2007, **96**, 2181–2196.

